NLO EVOLUTION KERNELS: MONTE CARLO VERSUS $\overline{\text{MS}}$* **

A. Kusina, S. Jadach, M. Skrzypek, M. Slawinska

The Henryk Niewodniczański Institute of Nuclear Physics
Polish Academy of Sciences
Radzikowskiego 152, 31-342 Kraków, Poland

(Received May 6, 2011)

We investigate the differences between the NLO evolution kernels in the Curci–Furmanski–Petronzio (CFP) and Monte Carlo (MC) factorization schemes for the non-singlet case. We show the origin of these differences and present them explicitly. We examine the influence of the choice of the factorization scale in the MC scheme (given by the upper phase space limit) on the evolution kernels in this scheme.

DOI:10.5506/APhysPolB.42.1475
PACS numbers: 12.38.–t, 12.38.Bx, 12.38.Cy

1. Introduction

Results presented in this contribution are needed for the exclusive modelling of the next-to-leading-order (NLO) DGLAP [1] evolution of the parton distributions in the Monte Carlo, see Refs. [2, 3, 4] for general scope of the project. In this approach the NLO evolution of the parton distributions is done by the Monte Carlo (MC) itself, with the help of newly defined *exclusive evolution kernels*. The important point is that the commonly used $\overline{\text{MS}}$ factorization scheme is not well suited for defining the exclusive kernels for the above MC modelling. For this purpose one needs to define a new factorization scheme, referred to in the following as the *Monte Carlo (MC) factorization scheme*, see Refs. [2, 3]. The calculations of the non-singlet NLO kernels (inclusive and exclusive) in this scheme have been presented in Ref. [5]. The properties of the new exclusive evolution kernels were also investigated in Refs. [6, 7].

* Presented by A. Kusina at the Cracow Epiphany Conference on the First Year of the LHC, Cracow, Poland, January 10–12, 2011.

** This work is supported by the Polish Ministry of Science and Higher Education grant No. 1289/B/H03/2009/37.

Why do we need a new factorization scheme? Traditional factorization theorems formulated in the early 1980s, see *e.g.* Refs. [8, 9, 10] separate collinear singularities only after the phase space integration, which is quite convenient for the analytical calculations. In the MC approach, however, it is unacceptable.

In defining the new MC factorization scheme classic works of Ellis, Georgi, Machacek, Politzer, Ross (EGMPR) [8] and Curci, Furmanski, Petronzio (CFP) [9] are used as a reference and a starting point. The definition of the new MC factorization scheme is not yet consolidated — it is still defined case by case, for more details see Refs. [2, 3, 5][1].

In the following, we shall concentrate on the standard inclusive evolution kernels in the MC factorization scheme focussing on the non-singlet DGLAP evolution. For more than two decades of the collider experiments the "industry standard" in the data analysis has been the $\overline{\text{MS}}$ factorization scheme. It is particularly suited for calculating the hard process matrix elements and PDFs and hence widely used. One of the essential properties of the $\overline{\text{MS}}$ is that it uses dimensional regularization, very convenient in the analytical calculations but rather unfriendly for the MC simulations. It is therefore necessary to compare the inclusive NLO DGLAP evolution kernels (depending only on the light-cone variable x and flavor indices) calculated in the $\overline{\text{MS}}$ and MC factorization schemes. This issue will be discussed in the following.

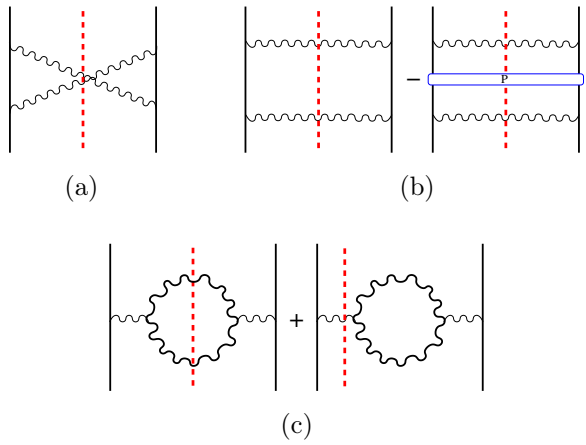

Fig. 1. A subset of Feynman cut-diagrams contributing to the non-singlet NLO DGLAP kernel: (a) ladder interference diagram, (b) double ladder diagram with counterterm, (c) gluon pair production diagrams: real and virtual.

[1] In the complementary approach of Refs. [11, 12, 13] soft singularities are resummed first and collinear resummation is added next.

In addition, we shall show how the choice of the type of the factorization scale in the MC scheme influences the inclusive kernels in this scheme. In the MC scheme, contrary to the $\overline{\rm MS}$, where factorization scale μ is a formal parameter, factorization scale is given by a kinematical variable enclosing the phase space from the above. The so-called evolution time variable used in the MC simulation is just a logarithm of this factorization scale.

Let us concentrate on a subset of cut-diagrams with two real partons contributing to the non-singlet NLO evolution kernel, in any scheme using axial gauge, see Fig. 1.

2. Notation and definitions

Our main intrest in this contribution are 2-real emission cut-diagrams, see Fig. 1. For the parametrization of the four-momentum of two emitted partons we use Sudakov variables

$$k_i^\mu = \alpha_i p^\mu + \beta_i n^\mu + k_{i\perp}^\mu\,, \qquad i=1,2\,, \tag{1}$$

where p is the four-momentum of the incoming quark and n is a light-cone vector (we use light-like axial gauge where $n^2=0$). In the massless limit of QCD we have $p^2 = k_i^2 = 0$, which fixes $\beta_i = -\frac{k_{i\perp}^2}{2\alpha_i(pn)} = \frac{\boldsymbol{k}_{i\perp}^2}{2\alpha_i(pn)}$. Additionally, we use symbol q for the off-shell momentum $q = p - k_1 - k_2$ and k for the sum $k = k_1 + k_2$.

Our preferred variables are related to polar angles of the emitted partons

$$\boldsymbol{a}_i = \frac{\boldsymbol{k}_{i\perp}}{\alpha_i}\,. \tag{2}$$

We refer to their modulus as the *angular scale* variables. They are related to rapidity via $\eta_i = \ln|\boldsymbol{a}_i| + \text{const}$.

The inclusive kernel in the CFP scheme [9] ($\overline{\rm MS}$) is defined as twice the residue in $\epsilon = 0$ of the bare PDF denoted as Γ [2]

$$\begin{aligned}\mathcal{P}(x) &= 2\,\mathrm{Res}_0\,\Gamma\,,\\ \Gamma &= x\,\mathrm{PP}\left[\frac{1}{\mu^{4\epsilon}}\int d\Psi\,\delta\left(x-\frac{qn}{pn}\right)Cg^4 W(k_1,k_2,\epsilon)\Theta(s(k_1,k_2)\leq Q)\right]\,.\end{aligned} \tag{3}$$

$d\Psi$ is a two particle phase space, $\delta\left(x-\frac{qn}{pn}\right) = \delta(1-x-\alpha_1-\alpha_2)$ defines the Bjorken x variable, C is a color factor, g is the strong coupling, $W(k_1,k_2,\epsilon)$ originates from the γ-trace of individual diagrams contributing to Γ, μ is a

[2] We skip the flavor indices as we are considering the non-singlet kernels, where nearly all diagrams contribute to the qq kernel.

formal energy scale of the $\overline{\rm MS}$ scheme — the factorization scale, term $\mu^{4\epsilon}$ originates from dimensional regularization in $n = 4+2\epsilon$ dimensions. Finally, the theta function $\Theta(s(k_1,k_2) \leq Q)$ defines the upper phase space limit for two emitted partons using a function of kinematical variables $s(k_1,k_2)$.

The definition of the inclusive kernel in the MC factorization scheme is similar

$$\begin{aligned} P(x) &= \frac{\partial}{\partial \ln Q} G(Q,x)\,, \\ G &= \int d\Psi \delta\left(x - \frac{qn}{pn}\right) xCg^4\, W(k_1,k_2,\epsilon=0)\Theta(Q > s(k_1,k_2) > q_0)\,. \end{aligned} \tag{4}$$

In this case the upper phase space limit Q plays the role of the factorization scale. As we shall see, changing the type of variable used as the factorization scale implies modification of the MC scheme. Typically, the factorization scale (upper limit) is defined in terms of angular scale variable $s(k_1,k_2) = \max\{|\boldsymbol{a}_1|, |\boldsymbol{a}_2|\}$ or transverse momentum $s(k_1,k_2) = \max\{|\boldsymbol{k}_{1\perp}|, |\boldsymbol{k}_{2\perp}|\}$. We shall refer to these two choices as angular ordering (a-ordering) and transverse momentum ordering ($k_\perp$-ordering).

We also introduced a lower cutoff q_0 for the purpose of regularization of the overall scale singularity (in CFP it is done in a dimensional manner). The distributions W of the CFP and MC schemes coincide in four dimensions, $W(k_1,k_2,\epsilon=0) = W(k_1,k_2)$.

In the analytical integration over the phase space in the calculation of the inclusive kernels the parametrization of the phase space is in practice fully determined by the choice of the phase space upper limit. For instance, if the angular variable is chosen, we also use it for the phase space parametrization

$$d\Psi_a = \frac{1}{4}\frac{\Omega_{1+2\epsilon}}{(2\pi)^{6+4\epsilon}}\frac{d\alpha_1}{\alpha_1}\frac{d\alpha_2}{\alpha_2}\alpha_1^{2+2\epsilon}\alpha_2^{2+2\epsilon} d\Omega_{1+2\epsilon} da_1 da_2 a_1^{1+2\epsilon} a_2^{1+2\epsilon}\,. \tag{5}$$

In the above an overall azimuthal angle dependence is already integrated out (only relative angle between emitted partons is kept). The same formula holds for the MC scheme in four dimensions ($\epsilon = 0$). In the case of $k_\perp$-ordering, the analogous parametrization reads

$$d\Psi_{k_\perp} = \frac{1}{4}\frac{\Omega_{1+2\epsilon}}{(2\pi)^{6+4\epsilon}}\frac{d\alpha_1}{\alpha_1}\frac{d\alpha_2}{\alpha_2} d\Omega_{1+2\epsilon} dk_{1\perp} dk_{2\perp} k_{1\perp}^{1+2\epsilon} k_{2\perp}^{1+2\epsilon}\,. \tag{6}$$

3. Single-logarithmic divergent diagrams

In this section, we show the general structure of single logarithmic divergent diagrams contributing to the NLO evolution kernel using the example of the ladder interference diagram of Fig. 1 (a), which we shall call Bx in

short. We analyze the integration procedure in the $\overline{\rm MS}$ scheme and in two MC schemes (with factorization scale in terms of angular scale variable and transverse momentum).

Choosing the upper phase space limit in terms of angular variable, the bare PDF (kernel) contribution of Bx diagram in the $\overline{\rm MS}$ factorization scheme reads

$$\begin{aligned}\Gamma_{Bx} = {\rm PP}\Bigg\{ & \left(\frac{\alpha_{\rm S}}{2\pi}\right)^2 \left(C_{\rm F}^2 - \tfrac{1}{2} C_{\rm A} C_{\rm F}\right) \frac{4}{\mu^{4\epsilon}} \frac{\Omega_{1+2\epsilon}}{(2\pi)^{2+4\epsilon}} \\ & \times \int \frac{d\alpha_1}{\alpha_1} \frac{d\alpha_2}{\alpha_2} (\alpha_1\alpha_2)^{2\epsilon} \delta(1-x-\alpha_1-\alpha_2) \int d\Omega_{1+2\epsilon} \\ & \times \int_0^\infty da_1 da_2 \frac{(a_1 a_2)^{1+2\epsilon}}{\tilde{q}^4(a_1,a_2)} T_{Bx}(a_1/a_2, \theta, \alpha_1, \alpha_2, \epsilon) \Theta(\max\{a_1,a_2\} \le Q) \Bigg\}, \quad (7)\end{aligned}$$

where T_{Bx} is a dimensionless function and $\tilde{q}^2 = \frac{1-\alpha_2}{\alpha_2} \boldsymbol{a}_1^2 + \frac{1-\alpha_1}{\alpha_1} \boldsymbol{a}_2^2 + 2\boldsymbol{a}_1 \cdot \boldsymbol{a}_2$. As it was already pointed out, Bx diagram features only single collinear divergence (single $\frac{1}{\epsilon}$ pole). This singularity can be isolated in the very beginning of the calculation (integration over the overall scale). It is done by means of introducing new integration (scale) variable using the identity $\Theta(\tilde{Q} > s(k_1,k_2)) \equiv \int_0^Q d\tilde{Q}\, \delta(\tilde{Q} = s(k_1,k_2))$, using at the same time dimensionless variables $y_i = \frac{a_i}{\tilde{Q}}$ Eq. (7) reads

$$\begin{aligned}\Gamma_{Bx} = {\rm PP}\Bigg\{ & \left(\frac{\alpha_{\rm S}}{2\pi}\right)^2 \left(C_{\rm F}^2 - \tfrac{1}{2} C_{\rm A} C_{\rm F}\right) \frac{4}{\mu^{4\epsilon}} \frac{\Omega_{1+2\epsilon}}{(2\pi)^{2+4\epsilon}} \\ & \times \int \frac{d\alpha_1}{\alpha_1} \frac{d\alpha_2}{\alpha_2} (\alpha_1\alpha_2)^{2\epsilon} \delta(1-x-\alpha_1-\alpha_2) \int_0^Q d\tilde{Q} \tilde{Q}^{4\epsilon-1} \int d\Omega_{1+2\epsilon} \\ & \times \int_0^1 dy_1 dy_2 \frac{(y_1 y_2)^{1+2\epsilon}}{\tilde{q}^4(y_1,y_2)} T_{Bx}(y_1/y_2, \theta, \alpha_1, \alpha_2, \epsilon)\, \delta(1-\max\{y_1,y_2\}) \Bigg\}. \quad (8)\end{aligned}$$

The overall scale singularity is now factorized in the form of the integral $\int_0^Q d\tilde{Q} \tilde{Q}^{4\epsilon-1} = \frac{Q^{4\epsilon}}{4\epsilon}$. If we perform the same calculation in the 4 dimensional MC factorization scheme, ($\epsilon = 0$) the scale singularity is regularized by means of a cutoff $\Theta(\max\{a_1,a_2\} > q_0)$. Then the integral containing the scale singularity takes the following form $\int_{q_0}^Q \frac{d\tilde{Q}}{\tilde{Q}} = \ln(Q/q_0)$.

Since Bx diagram does not feature additional collinear singularities we can perform the action of the pole part operator of the CFP scheme immediately and evaluate the remaining integrals in four dimensions. However,

there are still infra-red (IR) singularities originating from the integration over light-cone variables α. In the CFP scheme they are regularized in geometrical (non-dimensional) manner[3] and they do not contribute any additional collinear poles

$$\Gamma_{Bx} = \frac{1}{4\epsilon}\left(\frac{\alpha_{\rm S}}{2\pi}\right)^2 4\left(C_{\rm F}^2 - \tfrac{1}{2}C_{\rm A}C_{\rm F}\right)\int \frac{d\alpha_1}{\alpha_1}\frac{d\alpha_2}{\alpha_2}\delta(1-x-\alpha_1-\alpha_2)\int_0^{2\pi}\frac{d\phi}{2\pi}$$
$$\times \int_0^1 dy_1 dy_2 \frac{y_1 y_2}{\tilde{q}^4(y_1,y_2)} T_{Bx}(y_1/y_2,\theta,\alpha_1,\alpha_2,\epsilon=0)\delta(1-\max\{y_1,y_2\})\,. \quad (9)$$

In the MC scheme $\frac{1}{4\epsilon}$ gets replaced by $\ln(Q/q_0)$. It means that the inclusive (integrated) kernel contributions from Bx diagram (and also from all diagrams with only single collinear divergence) are the same in both the $\overline{\rm MS}$ and the MC scheme with angular factorization scale. A slight difference in the overall normalization is a matter of convention

$$P(x) = 2\mathcal{P}(x)\,. \quad (10)$$

What will happen if we change the type of the upper phase space limit? In Ref. [7] it was checked for the $\overline{\rm MS}$ scheme that the inclusive NLO kernels in this scheme do not depend on the choice of the upper limit (as expected). The question is now whether the same holds in the MC factorization scheme.

In the case of single logarithmic divergent (single $\frac{1}{\epsilon}$ pole) diagrams, like Bx, it is true again. It can be seen without performing the actual calculation — just by means of inspecting once again the calculation in the $\overline{\rm MS}$ scheme. We could write equation analogical to Eq. (7), but with the upper limit in terms of another variables, for instance using transverse momentum $\Theta(\max\{k_{1\perp},k_{2\perp}\}\leq Q)$. Next we would introduce dimensionless variables $y_i' = \frac{k_{i\perp}}{Q}$ and isolate once again the overall scale singularity. Since we consider diagrams free from internal $\frac{1}{\epsilon}$ poles we can take the residue or differentiate over $\ln(Q)$, obtaining the same result for both the $\overline{\rm MS}$ and MC schemes, independently of the type of the variable used in the MC scheme.

Summarizing, we have shown that the contribution to the NLO evolution kernel from the diagrams with single logarithmic divergence gives the same kernel contributions in all considered factorization schemes: the $\overline{\rm MS}$, MC with angular and transverse momentum factorization scale. Moreover, the

[3] The IR singularities in the CFP and MC schemes are regularized by principal value prescription: $\frac{1}{\alpha} \to \frac{\alpha}{\alpha^2+\delta^2}$. We also use the following notation of CFP for divergent integrals: $\int_0^1 d\alpha \frac{\alpha}{\alpha^2+\delta^2} \equiv I_0$ and $\int_0^1 d\alpha \ln\alpha \frac{\alpha}{\alpha^2+\delta^2} \equiv I_1$.

same argumentation will be applicable to the single logarithmic parts of the other diagrams. However, their double logarithmic parts will deserve special considerations, see below.

4. Double-logarithmic divergent diagrams

In this section, we consider the inclusive kernel contributions of the double logarithmic divergent (double pole) diagrams in the $\overline{\rm MS}$ and MC schemes. We use the example of the double ladder diagram (called Br) and its counterterm of Fig. 1 (b) and the gluon pair production diagrams (real and virtual) of Fig. 1 (c) (called Vg).

The double divergent diagrams are the sources of differences between inclusive kernels of $\overline{\rm MS}$ and MC schemes. The reason is that $\overline{\rm MS}$ kernels contain additional terms, originating from the artefacts of the dimensional regularization, generally form mixing $\epsilon \times \frac{1}{\epsilon^2} = \frac{1}{\epsilon}$ coming from additional ϵ terms in the phase space (kinematic) or in the γ-trace (spin).

4.1. Double ladder diagram and its counterterm

The structure of the kernel contribution of the double ladder graph (Br) is analogical to the one of the ladder interference diagram given in Eq. (7). In the case of the counterterm (Ct) the situation is slightly different due to the presence of additional projection operator. The calculations in the case of Br and its counterterm are more complicated and we do not present them explicitly in this contribution. We will present only the final results. For the details of the calculations we refer the reader to Ref. [5].

The inclusive kernel contribution of the double ladder graph and its counterterm in the $\overline{\rm MS}$ factorization scheme reads

$$\mathcal{P}_{Br-Ct}(x) = \left(\frac{\alpha_{\rm S}}{2\pi}\right)^2 C_{\rm F}^2 \left\{ \frac{1+x^2}{1-x} \left[-4I_0 - 4\ln(1-x) + 2\ln^2(x)\right] + 3(1-x)\left(1+\ln(x)\right) - (1+x)\left(\ln(x) + \tfrac{1}{2}\ln^2(x)\right) \right\}. \quad (11)$$

It does not depend on the choice of the upper phase space limit. The same kernel contribution in the MC scheme with angular factorization scale is the following

$$P^a_{Br-Ct}(x) = \left(\frac{\alpha_{\rm S}}{2\pi}\right)^2 C_{\rm F}^2 \left\{ \frac{1+x^2}{1-x} \left[-8I_0 - 8\ln(1-x) + 4\ln^2(x)\right] + (1-x)\left(6 - 2\ln(x)\right) - (1+x)\left(2\ln(x) - \ln^2(x)\right) \right\} \quad (12)$$

and in the MC scheme with transverse momentum factorization scale

$$P^{k_\perp}_{Br-Ct}(x) = \left(\frac{\alpha_S}{2\pi}\right)^2 C_F^2 \left\{ \frac{1+x^2}{1-x}\left[-8I_0 - 8\ln(1-x) + 4\ln^2(x)\right] \right.$$
$$\left. +(1-x)\left(6+2\ln(x)\right) - (1+x)\left(2\ln(x)+\ln^2(x)\right) \right\}. \quad (13)$$

The difference between the $\overline{\text{MS}}$ and MC schemes originates from the product of double pole $\frac{1}{\epsilon^2}$ and the coefficient terms expanded to $\mathcal{O}(\epsilon^1)$. There are two kinds of these terms. The first are from the phase space and depend on the type of the upper phase space limit (factorization scale in the MC scheme). The second are from the $\mathcal{O}(\epsilon^1)$ terms in the γ-trace and do not depend on the type of the factorization scale in the MC (spin part).

The difference between the $\overline{\text{MS}}$ and MC kernels written explicitly reads

$$P^s_{Br-Ct}(x) - 2\mathcal{P}_{Br-Ct}(x) = \mathcal{P}^{\text{Sp}}_{Br-Ct}(x) + \mathcal{P}^{\text{Kin }s}_{Br-Ct}(x)\,, \quad (14)$$

where index s indicates the type of the factorization scale in the MC scheme. The spin part of the difference is the same for all choices of factorization scales in the MC and reads

$$\mathcal{P}^{\text{Sp}}_{Br-Ct}(x) = -\left(\frac{\alpha_S}{2\pi}\right)^2 C_F^2\, 4(1-x)\ln(x)\,. \quad (15)$$

The kinematical difference is due to the choice of the upper phase space limit in the MC scheme. For the angular factorization scale it reads

$$\mathcal{P}^{\text{Kin }a}_{Br-Ct}(x) = \left(\frac{\alpha_S}{2\pi}\right)^2 C_F^2 \left[2(1+x)\ln^2(x) - 4(1-x)\ln(x)\right]. \quad (16)$$

For the transverse momentum factorization scale it vanishes

$$\mathcal{P}^{\text{Kin }k_\perp}_{Br-Ct}(x) = 0\,. \quad (17)$$

The kinematical difference is due to additional phase space factors in n-dimensions. For angular phase space of Eq. (5) it is the term $(\alpha_1\alpha_2)^{2\epsilon}$, which after expansion, multiplied by the double pole, contributes $2\epsilon\ln(\alpha_1\alpha_2)$ $\times\,\frac{1}{\epsilon^2}$ to the NLO DGLAP kernel. In the case of the transverse momentum phase space of Eq. (6) this kind of term is missing, *i.e.* $\mathcal{P}^{\text{Kin }k_\perp}_{Br-Ct}(x) = 0$.

The kinematical difference $\mathcal{P}^{\text{Kin }a}_{Br-Ct}(x)$ is also exactly equal the difference between kernel contributions in two MC schemes, one with angular and another with transverse momentum factorization scales

$$P^a_{Br-Ct}(x) - P^{k_\perp}_{Br-Ct}(x) = \left(\frac{\alpha_S}{2\pi}\right)^2 C_F^2 \left[2(1+x)\ln^2(x) - 4(1-x)\ln(x)\right]. \quad (18)$$

The above indicates that the $\overline{\rm MS}$ factorization scheme is *affine* with the MC scheme with transverse momentum factorization scale. Maximum $k_\perp$ is effectively representing a formal scale parameter μ (factorization scale) of the dimensional regularization in the $\overline{\rm MS}$. As was shown in Ref. [7] $\overline{\rm MS}$ kernels do not depend on the type of the upper phase space limit. If we choose phase space enclosing in form of another kinematical variable (not $k_\perp$), the additional $\sim \epsilon \times \frac{1}{\epsilon}$ terms in the $\overline{\rm MS}$ intervene and self-correct back to the case of transverse momentum. In the case of the 4-dimensional MC schemes there is no automatic self-correcting mechanism like in the $\overline{\rm MS}$ and kernels in the MC schemes with different types of the upper phase space limits will differ.

Summarizing, the "spin difference" between kernels in the $\overline{\rm MS}$ and MC schemes is the same, whereas the "kinematical difference" depends on the type of the upper phase space limit (factorization scale) in the MC scheme. For instance, for the factorization scale in terms of the light-cone minus variables $|\boldsymbol{k}_{i\perp}|/\sqrt{\alpha_i}$ the kinematical difference is due to the term $(\alpha_1\alpha_2)^\epsilon$ and reads

$$\mathcal{P}^{{\rm Kin}\,|\boldsymbol{k}_{i\perp}|/\sqrt{\alpha_i}}_{Br-Ct}(x) = \left(\frac{\alpha_{\rm S}}{2\pi}\right)^2 C_{\rm F}^2 \left[(1+x)\ln^2(x) - 2(1-x)\ln(x)\right] . \qquad (19)$$

The case of virtuality $(-q^2)$ upper limit was analyzed as well. The general result is the same, but the details of the calculations are a little bit more complicated.

4.2. Gluon pair production diagrams

The 2-real gluon pair production diagram (Vg) of Fig. 1 (c) features internal collinear singularity due to the production of a pair of collinear gluons. Analogous diagram with production of a quark–antiquark pair also contributes. As has been shown in Ref. [7], also in this case the $\overline{\rm MS}$ kernels do not depend on the choice of the upper limit. It is ensured (self-correction mechanism) by the corresponding virtual diagram of Fig. 1 (c).

The question is what happens in the 4-dimensional MC scheme? The internal collinear singularity leads to the double ϵ pole, which suggests that there could be a difference between kernel contributions in the MC schemes with different factorization scales. On the other hand, there is no additional projection operator as in the case of the double ladder graph and its counterterm, which suggests otherwise. In this case it is the virtual graph, which ensures the independence of the $\overline{\rm MS}$ kernel contribution on the type of the upper limit.

The real and virtual graphs are combined — this combination in the $\overline{\rm MS}$ and MC schemes is done in the same manner. Partial cancellation of the $\frac{1}{\epsilon^2}$ pole occurs, with the remnant giving rise to the running of the coupling

constant. It originates from the gluon self energy graph (the virtual graph in Fig. 1 (c)) from the integration of the term like $\ln(Q/\mu_R)$, where μ_R is the renormalization scale and Q is a kinematical variable to be chosen — the argument of the running coupling. The different choices of the running coupling argument Q do not affect the $\overline{\text{MS}}$ kernels, but they may affect the kernels in the MC schemes. The results of the preliminary studies indicate that if we choose the variable Q in terms of transverse momentum both the MC and $\overline{\text{MS}}$ schemes give the same results.

5. Conclusions

We investigated the differences between the non-singlet NLO DGLAP evolution kernels in the Curci–Furmanski–Petronzio scheme ($\overline{\text{MS}}$) and in the factorization scheme defined for the purpose of MC simulations. We show that the origin of these differences are due to the different definition of the projection operator in both schemes and examine explicitly the source of the differences.

We also examined the differences between MC schemes with factorization scales given in terms of rapidity related variables and transverse momentum, indicating the source of the differences explicitly. The type of the factorization scale in the MC scheme given by the upper phase space limit is related to the evolution time variable in the MC simulations. Knowing the differences between the kernels for different factorization scales is critical for understanding basic features of the MC factorization scheme and in particular what happens when switching between different evolution time variables in the MC simulation.

S.J. would like to acknowledge support and warm hospitality of CERN EP/TH and of the Baylor University.

REFERENCES

[1] L.N. Lipatov, *Sov. J. Nucl. Phys.* **20**, 95 (1975); V.N. Gribov, L.N. Lipatov, *Sov. J. Nucl. Phys.* **15**, 438 (1972); G. Altarelli, G. Parisi, *Nucl. Phys.* **126**, 298 (1977); Yu.L. Dokshitzer, *Sov. Phys. JETP* **46**, 64 (1977).

[2] S. Jadach *et al.*, `arXiv:1103.5015 [hep-ph]`.

[3] S. Jadach, M. Skrzypek, A. Kusina, M. Slawinska, *PoS* **RADCOR2009**, 069 (2010) [`arXiv:1002.0010 [hep-ph]`].

[4] S. Jadach, M. Skrzypek, *Acta Phys. Pol. B* **40**, 2071 (2009) [`arXiv:0905.1399 [hep-ph]`].

[5] S. Jadach, A. Kusina, M. Skrzypek, M. Slawinska, arXiv:1102.5083 [hep-ph].

[6] M. Slawinska, A. Kusina, *Acta Phys. Pol. B* **40**, 2097 (2009) [arXiv:0905.1403 [hep-ph]].

[7] A. Kusina, S. Jadach, M. Skrzypek, M. Slawinska, *Acta Phys. Pol. B* **41**, 1683 (2010) [arXiv:1004.4131 [hep-ph]].

[8] R.K. Ellis *et al.*, *Phys. Lett.* **B78**, 281 (1978).

[9] G. Curci, W. Furmanski, R. Petronzio, *Nucl. Phys.* **B175**, 27 (1980).

[10] J.C. Collins, D.E. Soper, G.F. Sterman, *Phys. Lett.* **B109**, 388 (1982).

[11] B.F.L. Ward, *Ann. Phys.* **323**, 2147 (2008) [arXiv:0707.3424 [hep-ph]].

[12] S. Joseph, S. Majhi, B.F.L. Ward, S.A. Yost, *Phys. Lett.* **B685**, 283 (2010) [arXiv:0906.0788 [hep-ph]].

[13] S. Joseph, S. Majhi, B.F.L. Ward, S.A. Yost, *Phys. Rev.* **D81**, 076008 (2010) [arXiv:1001.1434 [hep-ph]].